Jurnal Teknologi

Full Paper

THE PHITS SIMULATION STUDY FOR AN ALTERNATIVE PRODUCTION OF ^{32}P RADIOISOTOPE BY SECONDARY NEUTRON BOMBARDMENT OF ^{32}S TARGET

Suharni[a,b], Nunung Prabaningrum[b*], Imam Kambali[c]

[a]Research Center for Accelerator Technology, National Research and Innovation Agency, Tangerang Selatan, 15314, Banten, Indonesia
[b]Department of Nuclear Engineering and Engineering Physics, Gadjah Mada University, 55281, Yogyakarta, Indonesia
[c]Indonesian Nuclear Technology Polytechnic, National Research and Innovation Agency, Yogyakarta, 55281, Indonesia

Article history
Received
23 April 2024
Received in revised form
21 June 2024
Accepted
23 June 2024
Published Online
20 February 2025

*Corresponding author:
nunung.prabaningrum@ugm.ac.id

Graphical abstract

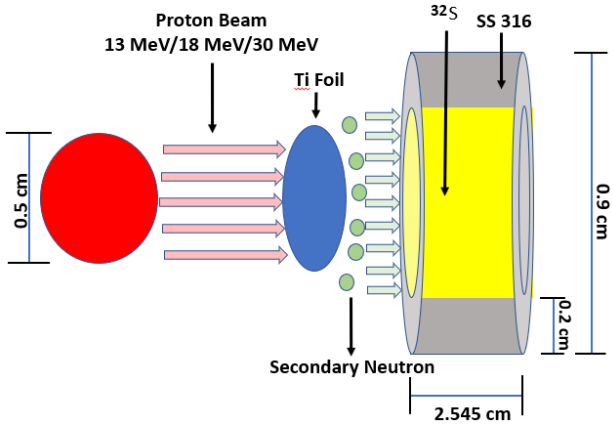

Abstract

Different methods of phosphorous-32 (^{32}P) radioisotope production have been of great interest over the past few years due to the wide range of ^{32}P applications in agriculture, health, and the environment. In this present study, using the PHITS simulation, ^{32}P radioisotope was theoretically produced by bombarding a natural sulfur target with secondary neutrons generated from 13, 18, and 30 MeV proton irradiation of Ti targets with thicknesses of 0.7, 1.2, and 3.0 mm, respectively. The calculated results showed that secondary neutron flux ranging from $1.78x10^{12}$ to $9.46x10^{12}$ n/cm^{2}s was generated from titanium-bombarded protons, which resulted in the ^{32}P radioactivity yields of 0.200, 0.840, and 3.167 MBq/μAh for proton energies of 13, 18, and 30 MeV, respectively. For 13 MeV protons, no radioactive impurity was generated during the bombardment, while radioactive impurities such as ^{31}Si, ^{30}P, ^{28}Al, and ^{31}S were produced from 30 MeV proton bombardment. The ^{32}P radioactivity yield s and the radioactive impurity yields increase further when the ^{32}S target is increased to 10 grams.

Keywords: ^{32}P radioisotope, PHITS simulation, proton beam, radioactivity yield, secondary neutron

1.0 INTRODUCTION

Over the past few decades, there has been a growing interest in research on radioisotope production as well as their applications in medicine, industry, agriculture, etc. One of the radioisotopes widely studied due to its various applications is phosphorus-32 (^{32}P) which decays by emitting beta particles with a maximum energy of 1.71 MeV, an average energy of 0.7 MeV, and a half-life of 14.3 days. In biological and medical research, ^{32}P is used for radiolabeling of DNA and RNA [1], for cancer cell treatment [2], for radiosynovectomy therapy [3], for emerging keloids therapy [4,5], as well as a murine melanoma treatment [6]. In agriculture, ^{32}P has been frequently employed to study fertilizer uptake by plants to

increase crop yields [7]. Radioisotope ^{32}P has also been applied in the field of soil and environment, such as for adsorption-desorption of phosphorus by lake sediments [8].

Due to its wide range of applications, effective and alternative methods for ^{32}P radioisotope production have been conducted and proposed. One of the methods for ^{32}P radioisotope production is by fast neutron irradiation of a sulfur or phosphorus target in a nuclear reactor. Vimalnath and co-workers produced ^{32}P radioisotope via $^{32}S(n,p)^{32}P$ and $^{31}P(n,\gamma)^{32}P$ nuclear reaction in a nuclear reactor with a neutron flux of up to 9.02 x 10^{11} and 7.8 x 10^{13} $cm^{-2}s^{-1}$ irradiated to a 250 g of ^{32}S and 0.35 g of ^{31}P targets respectively. Following the fast neutron irradiation for 88 days for the sulfur target and the thermal neutron irradiation for 63 days for the phosphorus target, they obtained a ^{32}P radioactivity yield of 165.4 GBq and 78.8 GBq respectively [9].

Researchers have recently proposed a novel method for radioisotope production using secondary neutron irradiation. The secondary neutrons which spectrum from low to fast neutrons were generated from a proton-bombarded primary target such as titanium [10], beryllium-titanium [11], as well as directly from enriched water target to theoretically [12] and experimentally [13] produce ^{64}Cu radioisotope. A vast number of neutron flux resulted from the interaction between proton beams and the primary targets indicating that radioisotopes could feasibly be produced by secondary neutron irradiation.

A team of researchers recently reported the possibility of ^{32}P radioisotope production using secondary neutrons from the $^{68}Zn(p,n)^{68}Ga$ reaction in a medical cyclotron [14]. The resulting radioactivity yield of ^{32}P was reportedly as much as 0.027 MBq/μAh for a 1-gram ^{32}S target. Based on the previous studies, the ^{32}P radioactivity yield may be increased by replacing the primary target with other targets to increase the secondary neutron flux. In this present study, we use the PHITS code to theoretically calculate the ^{32}P radioactivity yield by simulation of a 13, 18, and 30 MeV proton bombarded to a titanium target to produce ^{32}P radioisotope via $^{32}S(n,p)^{32}P$ reaction. Titanium is chosen as the primary target to generate secondary neutrons since its neutron yield is presumably high.

2.0 MATERIALS AND METHODS

In this present study, the PHITS 3.31 code [15] was used to calculate the radioactivity yields of ^{32}P as well as the radionuclide impurities that might be present during the bombardment. Three different proton energies, namely 13, 18, and 30 MeV were bombarded to a titanium (Ti) target with a diameter of 5 mm. The titanium target thicknesses were determined from the SRIM 2013 [16] calculations, which were 0.7, 1.2, and 3.0 mm for proton energy of 13, 18, and 30 MeV, respectively. In the PHITS simulation, a 40 μA proton beam current, which equals 2.5x10^{14} protons, was bombarded to the Ti foil for 1 hour. The protons and titanium foil interactions resulted in a vast number of secondary neutrons, which then the secondary neutron would hit the ^{32}S powder target placed in a stainless steel 316 (SS-316) body of 5 mm in inner diameter. The target geometry is shown in Figure 1.

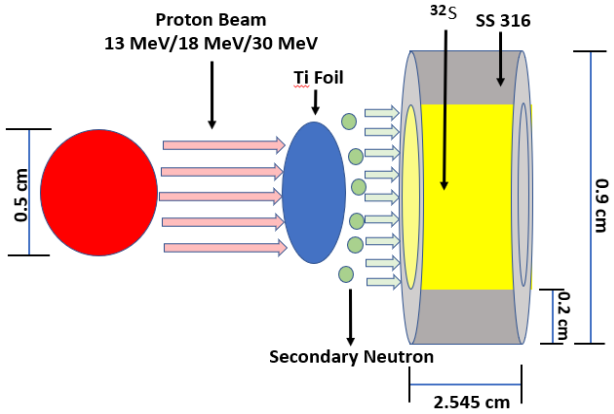

Figure 1 The target geometry employed in the PHITS code for 1-gram ^{32}S target

In the PHITS code, 1 gram of the ^{32}S target was placed in front of the Ti target without a distance, and the ^{32}S target thickness was around 25.45 mm or 2.545 cm. The irradiation time was determined from 1 to 5 hours, while the proton current was constant at 40 μA. The ^{32}P radioisotope yield was also calculated while the possible radioisotopic impurities were also evaluated from the simulation.

In this present work, the ^{32}S target mass was increased to 10 grams to study the influence of increasing the ^{32}S target thickness on the secondary neutron distribution, ^{32}P radioactivity yields, and the radioactive impurities. Therefore, the geometry of the PHITS code is depicted in Figure 2.

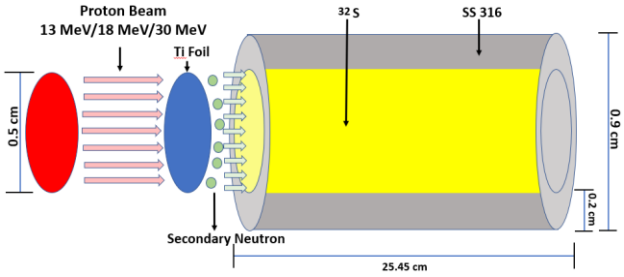

Figure 2 The target geometry employed in the PHITS simulation for the 10-gram ^{32}S target

The radioactive yields (*Y*) of ^{32}P radioisotope as well as all possible radioactive impurities during the neutron bombardment of the ^{32}S target were calculated by the following Equation [12]:

$$Y = \frac{mcN_A\,\sigma_T\phi}{A_T}(1 - e^{-\lambda t}) \quad (1)$$

where *m* = the target mass (g)

c = the isotope abundance
N_A = Avogadro's number
σ_T = total cross section (cm^2)
Φ = neutron flux (n/cm^2s^1)
A_T = atomic weight of the target material
λ = decay constant of the produced isotope (/s)
t = the irradiation time (s)

3.0 RESULTS AND DISCUSSION

3.1 Neutrons Spatial Distribution and Flux from 13, 18, and 30 MeV Proton-Bombarded Ti Target

Based on the PHITS simulation results of the 13-MeV protons incident on Ti target, the secondary neutrons distribute evenly along the y and z axes as shown in Figure 3, in which the blue color indicates neutron flux of 10^7 n/cm^2s while the red color depicts neutron flux of 10^{14} n/cm^2s. Note that the spatial distance between -1 to 3 cm is the observed section in the simulation. The secondary neutrons scatter in all directions, though the neutron flux is maximum around the Ti foil target, and then it decreases with the increasing distance relative to the Ti target position (0 cm). Since the ^{32}S target is only 2.545 cm long, it means that the ^{32}S target is entirely irradiated by neutrons, while a vast number of neutrons also pass through the ^{32}S target. This condition occurs when 18 and 30 MeV protons bombard the Ti target. In addition, the highest neutron flux of 10^{14} n/cm^2s scatter off the forward direction as indicated by the red color in front of the Ti target for all proton energies.

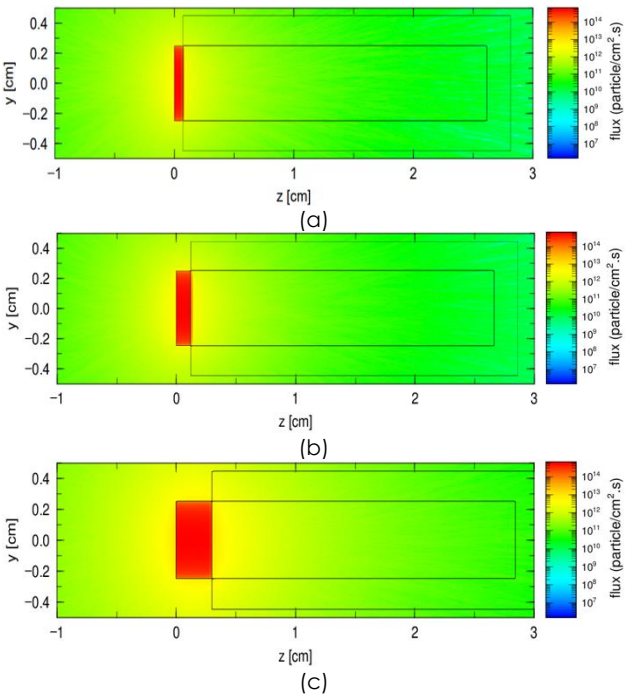

Figure 3 Spatial distribution of secondary neutron flux along the y and z axes when (a) 13 MeV, (b) 18 MeV, and (c) 30 MeV protons are bombarded to the Ti target, and the generated secondary neutrons then hit a 1 gram ^{32}S target

The calculated results also indicate that the neutron flux generated from the protons-bombarded Ti target increases with increasing incident proton energy from $1.78x10^{12}$ n/cm^2s for the 13 MeV incident protons to as high as $9.46x10^{12}$ n/cm^2s for the 30 MeV incident protons as listed in Table 1.

Table 1 Total neutron flux at different incident proton energies

Proton energy (MeV)	Total neutron flux (n/cm^2s)
13	$1.78x10^{12}$
18	$3.73x10^{12}$
30	$9.46x10^{12}$

3.2 ^{32}P Radioactivity Yields

Based on the PHITS calculations, when ^{32}P radioisotope is produced by secondary neutron irradiation as a result of a 13 MeV proton bombardment to a titanium target, the resulting radioisotope will only be ^{32}P or 100% of the product is ^{32}P radioisotope. However, the ^{32}P radioisotope product will slightly decrease to 99.85% when an 18 MeV proton beam is employed in the bombardment. The ^{32}P radioisotope product decreases dramatically to 64.81% should a 30 MeV proton beam be directed to the target as shown in Table 2. However, while the ^{32}P percentage declines with the increasing incident proton energy, the ^{32}P radioactivity yield remains higher since the total secondary neutron flux is higher.

For the 1 gram ^{32}S sample, the ^{32}P radioactivity yields for 13 MeV proton-irradiated target is 0.207 MBq/μAh, and then it goes up to 0.832 MBq/μAh for proton incident energy of 18 MeV. The radioactivity yield rises further to 3.279 MBq/μAh as the proton energy increases to 30 MeV.

Table 2 Radioactivity yields at different proton energies for 1-gram ^{32}S target

Proton energy (MeV)	Radioisotope products (percentage)	Nuclear reaction	Radioactivity yield (MBq/μAh)
13	^{32}P (100%)	$^{32}S(n,p)^{32}P$	0.207
18	^{32}P (99.85%)	$^{32}S(n,p)^{32}P$	0.832
30	^{32}P (64.81%)	$^{32}S(n,p)^{32}P$	3.279

3.3 Radioactive Impurities

Radioactive impurities are generated from neutron irradiation of the ^{32}S target, and they vary for different proton energies. Based on the PHITS calculations, different incident proton energies result in different radioisotope products as shown in Table 3. Surprisingly, no radioactive impurities are predictedly generated for the 13 MeV incident proton, whereas for the 18 MeV incident proton there are at least two significant radioactive impurities, namely ^{31}Si which originated from (n,2p) nuclear reaction, and ^{30}P which is due to

(n,p2n) nuclear reaction. ^{31}Si decays by emitting β^- radiation with a half-life of 157.24 minutes while ^{30}P is a β^+ particle emitting radioisotope with a half-life of 2.50 minutes. The radioactivity yields for both impurities are 1.914 and 0.032 Bq/μAh, respectively. These values are obtained from the PHITS simulation which can also be analytically calculated using Equation (1). Furthermore, the nuclear data, such as the half-lives and decay mode, can be found in previous publications [17].

Apart from ^{31}Si and ^{30}P radioisotopic impurities, more radioactive impurities could be present when the 30 MeV proton is used in the bombardment, including ^{28}Al which is presumably generated from (n,a) nuclear reaction, and ^{31}S which is a result of (n,2n) nuclear reaction. ^{28}Al is a radioisotope emitting β^- radiation with a half-life of 2.24 minutes, while ^{31}S is also β^- emitting radioisotope with a half-life of 2.55 seconds. It should be noted that for 30 MeV incident proton, the radioactivity yield for each predicted impurity is relatively high, which is up to 22.624 MBq/μAh for ^{31}S. Thus, radiation safety, separation, and purification should be taken with utmost consideration. Besides, according to the PHITS simulations, increasing the irradiation time to 5 hours would not change the types of radioactive impurities and yields.

Table 3 Radioactivity yields of radioactive impurities at different proton energies for 1-gram ^{32}S target

Proton energy (MeV)	Radioactive (percentage)	Half-life	Nuclear reaction	Radioactivity yield (Bq/μAh)	Decay mode
13	-	-	-	-	-
18	^{31}Si (0.15%)	157.24 min	^{32}S(n,2p)^{31}Si	1.914	β^-
	^{30}P	2.50 min	^{32}S(n,p2n)^{30}P	0.032	β^+
30	^{31}Si (33.02%)	157.24 min	^{32}S(n,2p)^{31}Si	2.262x10^5	β^-
	^{28}Al (9.4%)	2.24 min	^{32}S(n,a)^{28}Al	6.438x10^4	β^-
	^{30}P (5.78%)	2.50 min	^{32}S(n,p2n)^{30}P	3.958x10^4	β^+
	^{31}S (5.57%)	2.55 s	^{32}S(n,2n)^{31}S	3.818x10^4	β^-

3.4 Comparison with Previous Published Work

Based on the PHITS calculation results, The ^{32}P calculated radioactivity yield is much higher than previously published work by Tatari and co-workers [14] as shown in Table 4.

This higher yield is primarily due to higher secondary neutron flux generated from Ti foil than the ^{68}Zn target reported earlier [14]. This higher yield is largely due to the higher neutron flux generated from Ti foil compared to the ^{68}Zn target.

Moreover, the ^{32}P calculated radioactivity yield reported in this present work is slightly higher than the work published by Saied *et al*. [18]. Again, neutron flux greatly influences the ^{32}P calculated radioactivity yield.

Table 4 Comparison of this present work with other previously published works

Reference	Proton Energy (MeV)	Neutron-generated target	Neutron flux (n/cm^{2}s)	^{32}S radioactivity yield (MBq/μAh)
Saied, *et al*. [17]	20	-	1x10^{12}	0.800
Tatari, *et al*. [14]	10 -11	331.39 μm ^{68}Zn	5x10^8	0.027
This present work	13	1 mm Ti	1.78x10^{12}	0.207
	18		3.73x10^{12}	0.832
	30		9.46x10^{12}	3.279

3.5 Increasing ^{32}S Target Mass to 10 Grams

The target geometry was also changed to study the influence of ^{32}S target mass on the secondary neutron distribution, ^{32}P radioactivity yields, and the radioactive impurities. For a 10-gram ^{32}S target, the length of the target becomes 25.45 cm, while the observed section in the simulation is 250 cm. For the 10-gram ^{32}S target, the spatial distributions of the secondary neutrons as a result of the 13 MeV, 18 MeV, and 30 MeV proton bombardment are shown in Figures 4(a), 4(b), and 4(c), in which the blue color represents the neutron flux of 10^7 n/cm^{2}s, whereas the red color indicates the neutron flux of 10^{12} n/cm^{2}s.

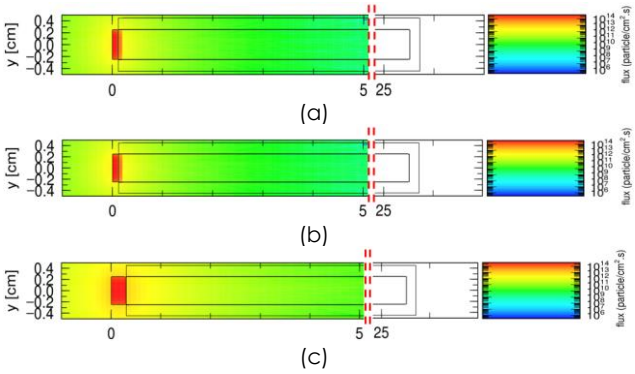

Figure 4 Spatial distribution of secondary neutron flux along the y and z axes when a 13-MeV (a), 18-MeV (b), and 30-MeV (c) protons are bombarded to the Ti target, and the generated secondary neutrons then hit a 10-gram ^{32}S target. Note that we cut the spatial distribution between 5 and 24 cm in the figure

As can be seen in Figure 4(a) – (c), the secondary neutron distributions are significantly different compared to the 1-gram ^{32}S target (see also Figs. 3(a) – (c)). The secondary neutrons generated from the 13-MeV, 18-MeV, and 30-MeV irradiated titanium foil cannot entirely pass through the 10-gram ^{32}S target, which is very different from the 1-gram ^{32}S target, where all neutrons can pass through the target.

Since the mass of the ^{32}S target increases to 10 grams, the ^{32}P radioactivity yield and radioactive impurity yield are expected to rise as shown in Tables 5 and 6, respectively. Increasing the ^{32}S target from 1 gram to 10 grams can increase the ^{32}P radioactivity yield by up to 6.33% for 13-MeV protons, 7.66% for 18-MeV protons, and 6.79%, respectively. The small increase in the ^{32}P radioactivity yields for all proton energies between 13 and 30 MeV is primarily due to the short range of the secondary neutrons in the 10-gram ^{32}S target. In other words, the 10-gram ^{32}S target blocks the neutrons to entirely pass through it.

Table 5 Radioactivity yields at different proton energies for 10-gram ^{32}S target

Proton energy (MeV)	Radioisotope products (percentage)	Nuclear reaction	Radioactivity yield (MBq/μAh)
13	^{32}P (100%)	$^{32}S(n,p)^{32}P$	0.221
18	^{32}P (99.85%)	$^{32}S(n,p)^{32}P$	0.901
30	^{32}P (64.81%)	$^{32}S(n,p)^{32}P$	3.518

While increasing the ^{32}S target from 1 gram to 10 grams can raise the ^{32}P radioactivity yield, however, the radioactive impurity yield also rises, even though no radioactive impurity remains observed for 13-MeV protons (see Table 5). The ^{31}Si radioactive impurity yield increases significantly up to 12.77% for a 30-MeV incident proton. Therefore, increasing the ^{32}S target to produce ^{32}P radioisotope might not be a good option since radioactive impurity yields rise significantly.

Table 6 Radioactivity yields of radioactive impurities at different proton energies for 10-gram ^{32}S target

Proton energy (MeV)	Radioactive (percentage)	Half-life	Nuclear reaction	Radioactivity yield (Bq/μAh)	Decay mode
13	-	-	-	-	-
18	^{31}Si (0.15%)	157.24 min	$^{32}S(n,2p)^{31}Si$	2.009	β^-
	^{30}P	2.50 min	$^{32}S(n,p2n)^{30}P$	0.034	β^+
30	^{31}Si (33.02%)	157.24 min	$^{32}S(n,2p)^{31}Si$	2.593×10^5	β^-
	^{28}Al (9.4%)	2.24 min	$^{32}S(n,a)^{28}Al$	7.302×10^4	β^-
	^{30}P (5.78%)	2.50 min	$^{32}S(n,p2n)^{30}P$	4.552×10^4	β^+
	^{31}S (5.57%)	2.55 s	$^{32}S(n,2n)^{31}S$	4.419×10^4	β^-

4.0 CONCLUSION

The production of a ^{32}P radioisotope using secondary neutrons emitted from proton bombardment on a titanium target has been theoretically calculated using the PHITS code. The secondary neutrons resulting from the proton-bombarded Ti targets range from 1.78 $\times10^{12}$ to 9.46$\times10^{12}$ n/cm^{2}s for proton energy 13 to 30 MeV. The ^{32}P radioactivity yield increases with increasing proton energy from 0.207 MBq/μAh for 13 MeV incident protons to 3.279 MBq/μAh for 30 MeV incident protons. The radioactive impurities vary with incident proton energies, in which no radioactive impurity is produced for 13 MeV proton incident energy. However, ^{31}Si and ^{30}P are predictably generated during 18 and 30 MeV proton bombardment, while other radioisotopic impurities such as ^{28}Al and ^{31}S are also present. Increasing the ^{32}S target mass from 1 gram to 10 grams results in higher ^{32}P radioactivity yield and radioactive impurity yields. These findings highlight that secondary neutrons generated from a proton-bombarded Ti foil can be used to produce a ^{32}P radioisotope. Further studies need to be conducted to increase the ^{32}P radioactivity yield while at the same time lowering the radioactive impurity yields.

Acknowledgment

The authors extend their gratitude to the Deputy of Human Resources for Science and Technology, National Research and Innovation Agency of Indonesia (BRIN) for their generous funding support, which has enabled the author (Suharni) to pursue studies under the Degree by Research scheme at the Master Program in Engineering Physics, Faculty of Engineering, Universitas Gadjah Mada.

Conflicts of Interest

The author(s) declare(s) that there is no conflict of interest regarding the publication of this paper.

References

[1] Creager, A. N. H. 2009. Phosphorus-32 in the Phage Group: Radioisotopes as Historical Tracers of Molecular Biology. *Stud. Hist. Philos. Biol. Biomed.* 40(1): 29–42.
[2] Cheng, Y., Kiess, A. P., Herman, J. M., Pomper, M. G., Meltzer, S. J., Abraham, J. M. 2015. Phosphorus-32, a Clinically Available Drug, Inhibits Cancer Growth by Inducing DNA Double-Strand Breakage. *Plos One*. 2015: 1–11.
[3] Knut, L. 2015. Radiosynovectomy in the Therapeutic Management of Arthritis. *World Journal of Nuclear Medicine*. 14(1): 10–15.
[4] Yan, D., Zhao, B., Yang, H., Zhu, B., Wang, J. 2013. A Combination of Nonoperative Treatment Modalities Used for Treatment of Keloids. *Dermatologic Therapy*. 27(1): 48–51.
[5] Ojeh, N., Bharatha, A., Gaur, U., Forde, A. L. 2020. Keloids: Current and Emerging Therapies. *Scars, Burns & Healing*. 6: 1–18.
[6] Salgueiro, M. J., Collia, N., Barreiro, M. L. A., Medina, V., Nicolini, J., Cremaschi, G., Zubillaga, M. 2009. Radioactive Treatment of a Murine Melanoma using a ^{32}P-patch. *Nucl. Med. Com.* 30: 706–712.
[7] Siyal, A. L., Hossain, A., Siyal, F. K., Jatt, T., Iram, S. 2022. Use of Radioisotopes to Produce High Yielding Crops in Order to Increase Agricultural Production. *Chem Proc*. 86: 1–11.

[8] Furumai H., Ohgaki, S., 1989. Adsorption-desorption of Phosphorus by Lake Sediments under Unaerobic Conditions. *Wat. Res*. 23(6): 677–683.
[9] Vilmanath, K. V., Shetty, P., Rajeswari, A., Chirayil, V., Chakraborty, S., Dash. A. 2014. Reactor Production of 32P for Medical Applications: An Assessment of 32S(n,p)32P and 31P(n,c) 32P Methods. *J. Radioanal. Nucl. Chem*. 2014: 1–12.
[10] Kambali, I., Febrianto, I. R. 2021. Feasibility Study of Copper-64 Radioisotope Production by Secondary Fast Neutron Bombardment. *IOP Conference Series: Earth and Environmental Science*. 927(1): 012034.
[11] Kambali, I., Febrianto, I., R., Ritawidya, R., Haryuni, D., R., Marlina, Nurhuda. 2023. On the Study of Cu-64 Production from 18 MeV Proton-induced Secondary Fast Neutron Bombardment. *Journal of the Korean Physical Society*. 82(4): 340–345.
[12] Auditore, L., Amato, E., Baldari, S. 2017. Theoretical Estimation of ^{64}Cu Production with Neutrons Emitted during ^{18}F Production with a 30 MeV Medical Cyclotron. *Appl. Radiat. Isot.* 122: 229–234.
[13] Alloni, D., Prata, M. 2017. Characterisation of the Secondary Neutron Field Generated by a Compact PET Cyclotron with MCNP6 and Experimental Measurements. *Appl. Radiat. Isot.* 128: 204–209.
[14] Tatari, M., Manshadi, Z. D., Naik, H. 2022. A Theoretical Study for the Production of ^{32}P Radioisotope using Neutrons from the ^{68}Zn(p,n)^{68}Ga Reaction in a Medical Cyclotron. *Appl/ Radiat. Isot.* 188: 110347.
[15] Sato, T., Y. Iwamoto, S. Hashimoto, T. Ogawa, T. Furuta, S.I. Abe, T. Kai, Y. Matsuya, N. Matsuda, Y. Hirata, T. Sekikawa, L. Yao, P.E. Tsai, H.N. Ratliff, H. Iwase, Y. Sakaki, K. Sugihara, N. Shigyo, L. Sihver, and K. Niita. 2024. Recent Improvements of the Particle and Heavy Ion Transport Code System - PHITS version 3.33. *J. Nucl. Sci. Technol*. 61(1): 127–135.
[16] Ziegler, J., F., Ziegler, M., D., Biersack, J., P. 2010. SRIM-The Stopping and Range of Ions in Matter. *Nucl. Instrum. Meth. Phys. Res. B.* 268: 1818–1823.
[17] Koning, A. J., D. Rochman, J.-Ch. Sublet, N. Dzysiuk, M. Fleming, and S. van der Marck. 2019. TENDL: Complete Nuclear Data Library for Innovative Nuclear Science and Technology. *Nucl. Data Sheets.* 155: 1–55.
[18] Saied, B. M., Naji, N. F., Abd Al-Ameer, A. L. M. 2015. Yields for the Production of Phosphorus-32 using the Charged and Uncharged Particles in Medical Practice. *Int. J. Med. Pharmaceut. Sci.* 5: 67–76.